

# The Displacement Response Study for Different Graded Parameter Functionally Graded Materials Based on Strip Element Method

**†J.H. Tian, L.L. Ma**

(CAE Analysis Room for Engineering Application ,School of Mechatronic Engineering ,Xi'an Technological  
University, Xi'an 710021 China)

†Correspondence to: J.H .Tian, School of Mechatronic Engineering , Xi'an Technological  
University, Xi'an 710021 China.

†Corresponding author: 540673737@qq.com

## Abstract

In this paper, the displacement response of functionally graded material structure under mechanical loading was studied by using strip element method. Established a parameterized model for describing the functional gradient material physical properties, the displacement expression of strip element method was deduced, using the virtual work principle to get the control equations of functionally graded materials plane problem, using the modal superposition method to complete the solution of the equation. The accuracy of the calculation method was verified by comparison with the result of finite element method. The research shows that the results of the strip element method are consistent with the finite element method in the displacement response of the functionally graded materials under mechanical loading. With the increase of the gradient coefficient, the ceramic content is increased, and the material stiffness is also increased, then the structure response caused by external loading is decreased. With the increase of the gradient coefficient, the influence of the gradient coefficient to the structure displacement response is decreased gradually.

**Keyword:** Displacement Response; Functionally Graded Materials; Strip Element Method.

## 1 Introduction

Functional gradient material is a kind of polyphase material, which continuously controls the distribution of components in the preparation of materials so as to meet different requirements of different parts of the structure [1][2]. At the same time due to material and components of continuous changes in the structure, there is no macro interface, avoid the traditional composite interface place due to the performance of the mutation and the damage was caused by the occurrence of failure [3]. Functional gradient materials can be designed to change the distribution of material components and bring the development of composite materials to a new level.

In recent years, experts and scholars had conducted in-depth study on the mechanical problems of functionally graded materials. The free vibration of functional gradient materials under mechanical loading and temperature loading was analyzed using Peano-Baker series method by Liu Wuxiang[4]. The dynamic characteristic analytical solution of the quadrilateral and rhombic function gradient plate was obtained by using the beam function group [5]. Reddy [6] adopted the first-order shear deformation theory to study the structural response of the functional gradient plate structure under the thermo-machine coupling. Using the first-order shear deformation theory, Thai [7] had studied the problem of bending and free

vibration of functionally graded materials. Liew [8] studied the vibration response of functionally graded material plates under the coupling of mechanical load and electromagnetic load based on the first-order shear deformation theory using the finite element method. Zenkour [9] used first-order shear deformation theory and classical elastic theory to study the structural bending deformation of the sandwich structure under mechanical loading. Ferreira [10] used three-order shear deformation theory and meshless method to study the structure response of functional gradient materials under static load. Reddy [11] studied the deformation of functional gradient rectangular plate based on the three-order shear deformation theory. Brischetto [12] studied the analytic solution of the structural displacement response of functionally graded material plates under transverse loading. Ray [13] used the finite element method to study the structural response of the functional gradient fiber piezoelectric materials in exponential distribution. Kulikov [14] adopted surface sampling method to solve the problem of three-dimensional thermal stress of functional gradient materials.

Due to physical performance parameters of functionally gradient materials with the coordinate changing continuously, the constant coefficient differential equation turns into the variable coefficient differential equation while the theory of elastic body deformation is derived, it is difficult to solving such problem by analytical method. The numerical method is used to solve complex problem while the large computation is in process. In recent years, the researchers have proposed a semi-numerical and semi-analytic method, that is called the strip element method [15]. It uses the merit of analytical method and numerical method for widely used.

## 2 Strip element method theory

The strip element method is a series of strip element separated by the solution domain as shown in fig.1. The displacement function is the continuous function of  $x$ , and the displacement of the element is obtained through the line displacement interpolation.

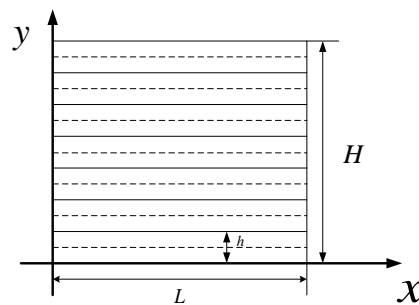


Fig.1 strip element method for solving model

It is assumed that the displacement functions of functionally graded materials under external loads are

$$U = N(y)V(x)\exp(-i\omega t) \quad (1)$$

where  $N(y)$  represents shape function for displacement interpolation;  $V(x)$  represents displacement function;  $\omega$  represents circle frequency;  $t$  represents time.

The expression of  $N(y)$  is

$$N(y) = \begin{bmatrix} (1 - \frac{3y}{h} + 2\frac{y^2}{h^2})\mathbf{I} & 4(\frac{y}{h} - 4\frac{y^2}{h^2})\mathbf{I} & (-\frac{y}{h} + 2\frac{y^2}{h^2})\mathbf{I} \end{bmatrix} \quad (2)$$

where  $h$  represents element thickness;  $\mathbf{I}$  represent 2 order element matrix. According to Kausel 's equation, the equilibrium equation of the system is

$$\rho\ddot{U} - L^T \sigma = 0 \quad (3)$$

where  $U$  represents displacement vector;  $L$  represent differential operator matrix;  $\sigma$  represents stress vector and  $\sigma = [\sigma_x \ \sigma_y \ \tau_{xy}]^T$ ; superscript  $T$  denotes transpose.

Where the expression for  $L$  is

$$L = \begin{bmatrix} \frac{\partial}{\partial x} & 0 \\ 0 & \frac{\partial}{\partial y} \\ \frac{\partial}{\partial y} & \frac{\partial}{\partial x} \end{bmatrix} \quad (4)$$

The displacement function is introduced into (3), given

$$W = \rho\ddot{U} - L^T \sigma \quad (5)$$

Since the internal displacement function of the element is interpolated by the nodal displacement, the residual value must be exist in the element, then  $W \neq 0$

By the principle of virtual work, there is

$$\delta V(x)^T F = \delta V(x)^T S + \int_0^h \delta U^T W dy \quad (6)$$

Where  $F$  represents external mechanical load;  $S$  represent nodal stress vector.

Given an external load as

$$F = \overline{F} \exp(-i\omega t) \quad (7)$$

where  $\overline{F}$  represents external load amplitude.

The element stress is

$$S^T = [R_x^T \Big|_{y=0} \quad R_x^T \Big|_{y=\frac{h}{2}} \quad R_x^T \Big|_{y=h}] \quad (8)$$

where stress  $R_x$  is

$$R_x = L_x^T cLU \quad (9)$$

where  $L_x = \begin{bmatrix} 1 & 0 & 0 \\ 0 & 0 & 1 \end{bmatrix}$ ;  $c$  is the elastic constant matrix  $c = \begin{bmatrix} c_{11} & c_{12} & c_{13} \\ c_{21} & c_{22} & c_{23} \\ c_{31} & c_{32} & c_{33} \end{bmatrix}$

The displacement expression is substituted into the virtual work equation and we obtain

$$\bar{F} = -A_2 \frac{\partial^2 V(x)}{\partial x^2} + A_1 \frac{\partial V(x)}{\partial x} + A_0 V(x) - \omega^2 M V(x) \quad (10)$$

where  $A_0$ ,  $A_1$  and  $A_2$  represent coefficient matrix.  $M$  represents mass matrix.

It can be seen from the equation (10) that the governing equation obtained by element discretization is the ordinary differential equation of  $x$ , which reduces the difficulty of the solution, it also reflects the idea of  $y$  direction discretization.

The coefficient matrix is

$$A_0 = \frac{1}{3h} \begin{bmatrix} 7D_{xx} & -8D_{xx} & D_{xx} \\ -8D_{xx} & 16D_{xx} & -8D_{xx} \\ D_{xx} & -8D_{xx} & 7D_{xx} \end{bmatrix} \quad (11)$$

$$A_1 = \frac{1}{3} \begin{bmatrix} 3(D_{xy} - D'_{xy}) & -4D_{xy} & D_{xy} \\ 4D_{xy} & 0 & -4D_{xy} \\ -D_{xy} & 4D_{xy} & 3(D_{xy} - D'_{xy}) \end{bmatrix} \quad (12)$$

$$A_2 = \frac{h}{30} \begin{bmatrix} 4D_{yy} & 2D_{yy} & -D_{yy} \\ 2D_{yy} & 16D_{yy} & 2D_{yy} \\ -D_{yy} & 2D_{yy} & 4D_{yy} \end{bmatrix} \quad (13)$$

where

$$D_{xx} = \begin{bmatrix} c_{11} & c_{13} \\ c_{13} & c_{33} \end{bmatrix}; \quad D_{yy} = \begin{bmatrix} c_{33} & c_{23} \\ c_{23} & c_{22} \end{bmatrix}; \quad D_{xy} = \frac{1}{2} \begin{bmatrix} 2c_{13} & c_{33} + c_{12} \\ c_{33} + c_{12} & 2c_{23} \end{bmatrix}; \quad D'_{xy} = \begin{bmatrix} c_{13} & c_{12} \\ c_{33} & c_{23} \end{bmatrix}$$

The expression for the mass matrix is

$$M = \int_0^h \rho N(y)^T N(y) dy \quad (14)$$

Assemble all the elements in the domain of the problem, and the differential equation is obtained in the whole domain.

$$\bar{F}_t = [-A_{2t} \frac{\partial V_t(x)}{\partial x^2} + A_{1t} \frac{\partial V_t(x)}{\partial x} + A_{0t} V_t(x) - \omega^2 M_t V_t(x)] \quad (15)$$

where  $A_{0t}$ ,  $A_{1t}$  and  $A_{2t}$  are the coefficients matrix for the element assembly in the solving domain;  $M_t$  is the mass assembly matrix;  $\bar{F}_t$  is the external mechanical load;  $V_t(x)$  is the displacement function in the solving domain.

Assumed the displacement function form is

$$V_t(x) = d_t \exp(ikx) \quad (16)$$

Assumed external mechanical load form is

$$\overline{F}_t = P_t \exp(ikx) \quad (17)$$

The equation (16), (17) substitution into equation (15), we obtain

$$P_t = [k^2 A_{2t} + ikA_{1t} + A_{0t} - \omega^2 M_t] d_t \quad (18)$$

$P_t$  represents the load acting on the nodal line, while  $P_t = 0$  the equation (18) is transformed into a homogeneous equation, and the eigenvalue equation for the  $k$  is obtained.

$$[k^2 A_{2t} + ikA_{1t} + A_{0t} - \omega^2 M_t] d_t = 0 \quad (19)$$

Equation (19) can be written

$$\left( \begin{bmatrix} 0 & \mathbf{I} \\ \omega^2 M_t - A_{0t} & -iA_{1t} \end{bmatrix} - k \begin{bmatrix} \mathbf{I} & 0 \\ 0 & A_{2t} \end{bmatrix} \right) \begin{Bmatrix} d_t \\ kd_t \end{Bmatrix} = 0 \quad (20)$$

The  $2M$  ( $M=6N-2(N-1)=4N-2$ ) eigenvalue is obtained by solving the equation (20), and the eigenvectors corresponding to the  $j$ th eigenvalues are represented as  $\phi_j$

$$\phi_j = [\phi_{1,j} \quad \phi_{2,j} \cdots \phi_{M,j}] \quad (21)$$

By means of the modal superposition method, the solution of the equation can be expressed as

$$V_t = \sum_{j=1}^{2M} C_j \phi_j \exp(ik_j x) = G(x)C \quad (22)$$

where

$$G(x) = \begin{bmatrix} \phi_{1,1} X_1 & \phi_{1,2} X_2 & \cdots & \phi_{1,2M} X_j \\ \phi_{2,1} X_1 & \phi_{2,2} X_2 & \cdots & \phi_{2,2M} X_j \\ \vdots & \vdots & \ddots & \vdots \\ \phi_{M,1} X_1 & \phi_{M,2} X_2 & \cdots & \phi_{M,2M} X_j \end{bmatrix} \quad (23)$$

$$X_j = \exp(ik_j x) \quad (24)$$

Equation (22) is a fundamental solution of the equation. There are  $2M$  constants  $C$  in this fundamental solution, so it is necessary to determine the unknown coefficients by the boundary conditions.

Since equation (22) is the fundamental solution in the problem domain, the displacement at any point satisfies the equation (22), and the displacement is satisfied at the right boundary of the solution.

$$V_{bt}^R = \sum_{j=1}^{2M} C_j \phi_j \exp(ik_j x^R) = G(x^R)C \quad (25)$$

That can be written

$$G(x^R)C = V_{bt}^R \quad (26)$$

The same way, on the left side

$$G(x^L)C = V_{bt}^L \quad (27)$$

The equation (26) and (27) are assembled and sorted, and the constant  $C$  expression can be obtained

$$C = G_d^{-1} V_{bt}^T = \begin{bmatrix} G(x^R) \\ G(x^L) \end{bmatrix}^{-1} V_{bt}^T \quad (28)$$

Where  $V_{bt}$  is the displacement at the boundary

$$V_{bt} = \begin{bmatrix} V_{bt}^R & V_{bt}^L \end{bmatrix} \quad (29)$$

By equation (23),  $G(x^R)$  can be expressed as

$$G(x^R) = \begin{bmatrix} \phi_{11} X_1^R & \phi_{12} X_2^R & \cdots & \phi_{1L} X_j^R \\ \phi_{21} X_1^R & \phi_{22} X_2^R & \cdots & \phi_{2L} X_j^R \\ \vdots & \vdots & \ddots & \vdots \\ \phi_{M1} X_1^R & \phi_{M2} X_2^R & \cdots & \phi_{ML} X_j^R \end{bmatrix} \quad (30)$$

$$X_j^R = \exp(ik_j x^R) \quad (31)$$

The superscript  $R$  represents the right boundary.

Similarly, the left boundary condition has the same form as the displacement matrix at the right boundary. The difference between the two forms is that the  $x$  coordinate value at the right boundary is changed to the  $x$  coordinate value at the left boundary.

$$X_j^L = \exp(ik_j x^L) \quad (32)$$

### 3 Application of the boundary conditions

The stress vector of the internal element can be expressed as

$$R_x = D_{xx} \frac{\partial U}{\partial x} + D_{xy} \frac{\partial U}{\partial y} \quad (33)$$

The displacement function is substituted

$$R = R_1 V(x) + R_2 \frac{\partial V(x)}{\partial x} \quad (34)$$

Where  $R_1$  and  $R_2$  are element coefficient matrices  
 $R_1$  is

$$R_1 = \frac{1}{h} \begin{bmatrix} D_{yy} & -4D_{yy} & 3D_{yy} \\ -D_{yy} & 0 & D_{yy} \\ -3D_{yy} & 4D_{yy} & -D_{yy} \end{bmatrix} \quad (35)$$

$R_2$  is

$$R_2 = \begin{bmatrix} D_{yx}' & 0 & 0 \\ 0 & D_{yx}' & 0 \\ 0 & 0 & D_{yx}' \end{bmatrix} \quad (36)$$

Calculate the  $R_1$  and  $R_2$  for all elements, and obtain the overall stress vector  $R_t$  as follows

$$R_t = R_{1t} V_t(x) + R_{2t} \frac{\partial V(x)}{\partial x} \quad (37)$$

where  $R_{1t}$ ,  $R_{2t}$  is the assemble matrix of the element coefficient matrix.

The displacement is simplified by using the left and right boundaries

$$\frac{\partial V(x)}{\partial x} = \sum_{j=1}^{2M} ik_j \exp(ik_j x) \cdot c_j = G' \cdot C = G' \cdot G_d^{-1} V_{bt} \quad (38)$$

The stress vector of the inner nodal line is equal to the average value of the stress vector of the adjacent left and right elements. We obtains

$$R_{bt} = K V_{bt} \quad (39)$$

In the equation,  $R_{bt} = \begin{bmatrix} R_{bt}^R & R_{bt}^L \end{bmatrix}$  is an external load acting on the left and right boundaries, where the stiffness matrix  $K$  is

$$K = \begin{bmatrix} R_{1t} & 0 \\ 0 & R_{2t} \end{bmatrix} + \begin{bmatrix} R_{2t} G^{R'} G_d^{-1} \\ R_{2t} G^{L'} G_d^{-1} \end{bmatrix} \quad (40)$$

In equation (40),  $G^{R'}$  and  $G^{L'}$  have the same expressions as  $G^R$  and  $G^L$ . The difference is that  $G^R$  and  $G^L$  in  $X_j^R$  and  $X_j^L$  are replaced by  $X_j^{R'} = ik_j \exp(ik_j x^R)$  and

$X_j^{L'} = ik_j \exp(ik_j x^L)$  respectively.

Equation (39) reflects the relationship between the stress boundary condition and displacement, the stress and displacement boundary conditions are transformed into displacement boundary conditions by equation (39), a constant  $c$  can be obtained by substituting the boundary displacement into equation (28), from equation (22) and (1) the displacement can be obtained in the solving problem.

#### 4 Establishment of gradient parameter model

The functional gradient materials studied in this paper are composited by metal and ceramic materials. The metal material is  $1Cr_{18}Ni_{11}Nb$  and the ceramic material is  $Si_3N_4$ . The physical properties of the two materials are shown in table 1.

Tab.1 physical properties of  $1Cr_{18}Ni_{11}Nb$  and  $Si_3N_4$  materials

material	Modulus of elasticity / MPa	Poisson' s ratio
$1Cr_{18}Ni_{11}Nb$	$2.38 \times 10^5$	0.3177
$Si_3N_4$	$3.22 \times 10^5$	0.2400

Because functionally graded materials are continuously changed by different materials according to the design requirements, the physical performance parameters of the materials are expressed as a function of the volume fraction of the material, the physical properties of the materials and the content of components, it denotes as

$$\begin{aligned}
 E(y) &= (E_C - E_M)Q_C + E_M \\
 \nu(y) &= (\nu_C - \nu_M)Q_C + \nu_M \\
 \rho(y) &= (\rho_C - \rho_M)Q_C + \rho_M
 \end{aligned} \tag{41}$$

where  $E(y)$ ,  $\nu(y)$  and  $\rho(y)$  are the elastic modulus, Poisson's ratio and density of FGM plates, respectively.  $E_C, \nu_C$  and  $\rho_C$  are the elastic modulus, Poisson's ratio and density of ceramic materials, respectively.  $E_M, \nu_M, \rho_M$  are the elastic modulus, Poisson's ratio and density of metal materials, respectively.  $Q_C$  is the volume fraction of the ceramic.

To ensure the continuity of the material, the sum of the metal volume fraction and the ceramic volume fraction at any location of the material is 1.

$$Q_C + Q_M = 1 \tag{42}$$

where,  $Q_M$  is the volume fraction of metals.

The volume fraction change function of the functionally graded metal is

$$Q_M = \left(1 - a\left(1 - \frac{y}{H}\right) + b\left(1 - \frac{y}{H}\right)^c\right)^p \quad (43)$$

where  $y$  is the vertical position and  $0 \leq y \leq H$ ;  $H$  is FGM plate thickness;  $p \geq 0$  is the gradient parameters.

By equation (43), it can be seen that when  $p=0$ ,  $Q_M=1$ , and  $Q_C=0$ . Substituting that into (41) we have  $E(y) = E_M$ ,  $\nu(y) = \nu_M$ ,  $\rho(y) = \rho_M$  and functionally graded material degenerates into pure metal homogeneous material, When  $p$  tends to infinity, the  $Q_C$  tends to 1, and the equation (41) can be obtained  $E(y) = E_C$ ,  $\nu(y) = \nu_C$ ,  $\rho(y) = \rho_C$ , and the material is reduced to a pure ceramic homogeneous material.

When  $a=1$  and  $b=0$  are functionally graded materials, the volume fraction of metals varies as shown in Figure 2

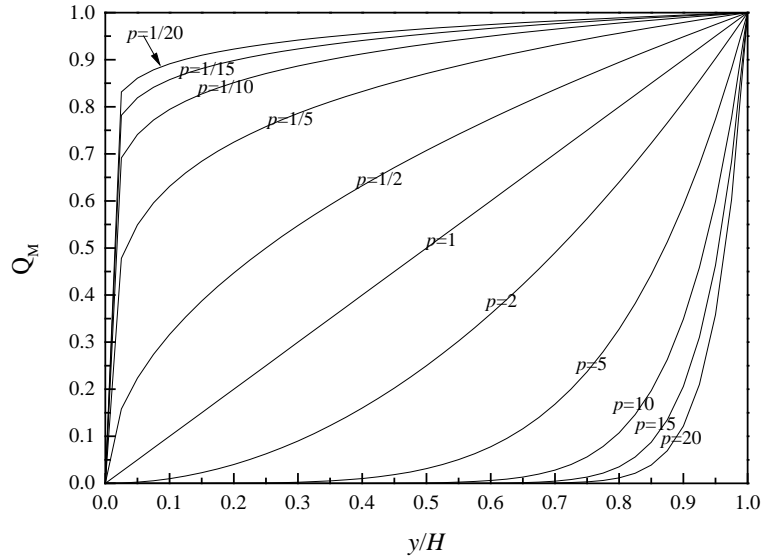


Fig. 2 law of change of volume fraction of metal with thickness under different gradient parameters at  $a=1$  and  $b=0$

The figure 2 can be shown, when  $y = 0$ , metal volume fraction is 0, this position is pure ceramic material, when  $y = H$ , metal volume fraction is equal to 1, this position is the pure metal homogeneous material. So when  $a = 1$ ,  $b = 0$ , the transition form of materials is a continuous transition of ceramic to metal. When the gradient parameter  $p = 1$ , the change of the volume fraction of the functionally graded material is continuous linear change. When the gradient parameter is lesser than 1, the change of the metal volume fraction decreases. When the gradient parameter is greater than 1, the metal volume fraction of the functional gradient material is slower in the early, then the volume fraction is accelerated with the thickness increased.

## 5 computational model

### 5.1 Validation of strip element method

The model of figure 3 is solved by using the strip element method. In figure 3,  $L = 100\text{mm}$ ,  $H$

= 100mm, the lower boundary is fixed,  $q = 100\text{N/mm}$  uniform load is applied on the upper boundary. The solution domain is divided into 20 elements and the material properties in each element are metal material. The metallic material property is shown in table 1. The displacement at  $y = 10\text{mm}$ ,  $y = 50\text{mm}$ , and  $y = 90\text{mm}$  is shown in figure 4 by strip element method and finite element method.

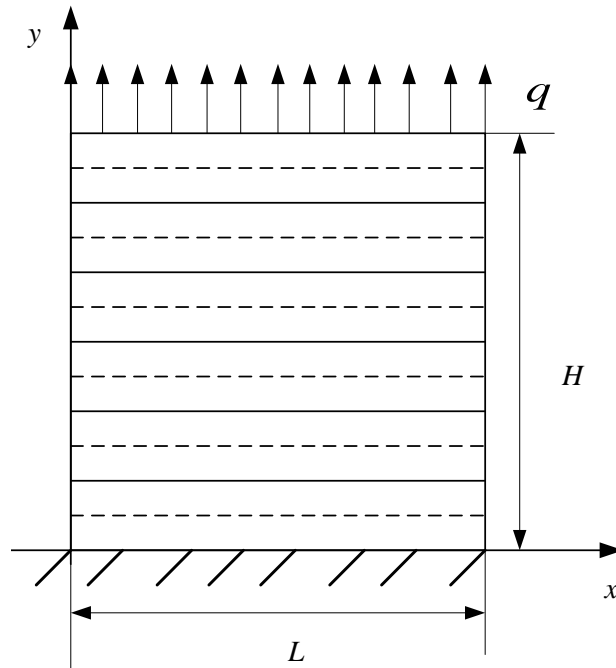


Fig. 3 physical model of plane problem

From fig.4 we can see that the displacement obtained by strip element method and finite element method in  $y$ -direction at different position is almost the same. From  $y = 10\text{mm}$ ,  $y = 50\text{mm}$ , to  $y = 90\text{mm}$ , the displacement in  $y$ -direction is increased. The accuracy of the strip element method is verified.

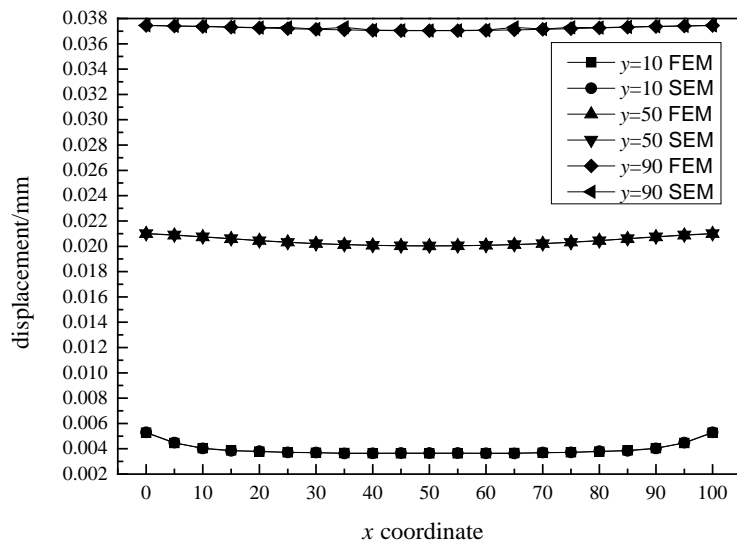


Fig. 4 the displacement in y-direction in different position by FEM and SEM

### 5.2 The influence of element number for the results

In the calculation process, because of the discrete of the solving domain, the size of the element has an influence on the accuracy of the displacement solution. Figure 5 and figure 6 are the  $x$ -direction displacement and the  $y$ -direction displacement at  $y=10\text{mm}$  using 10 elements, 20 elements and 50 elements, respectively. It can be known that displacement results have small difference when the element number is 10 and 20, while when the element number is 20 and 50, the result difference is not obvious, so in this calculation the element number is set to 20 for ensuring that precision and calculation speed.

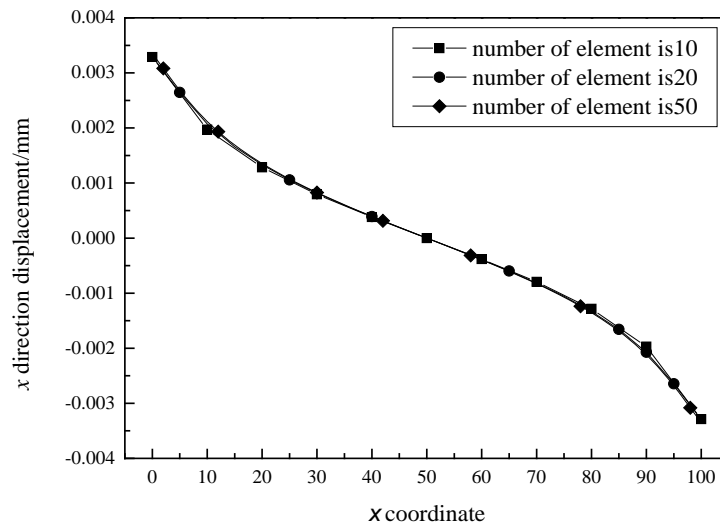


Fig. 5 calculation results of  $x$  direction displacement at  $y=10\text{mm}$

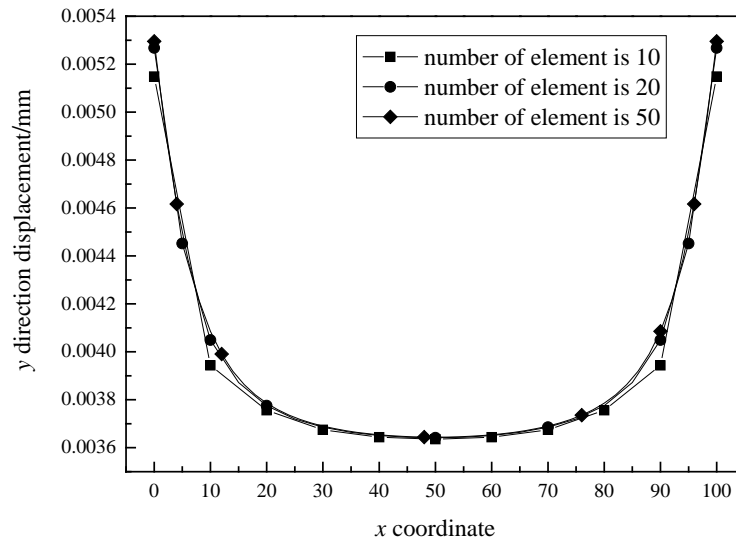


Fig. 6 calculation results of  $y$  direction displacement at  $y=10\text{mm}$

### 5.3 Structural response analysis of functionally graded materials

The displacements with different gradient parameters are shown in figure 7 at  $y = 10\text{mm}$  in the  $x$  direction. It can be seen from figure 7, with the increase of gradient coefficient, the

displacement response decreases, and this is due to metal volume fraction decreases in the functionally graded materials, ceramic volume fraction increases, causing the structure stiffness increased. In addition, the displacement in the  $x$  direction at  $y = 10\text{mm}$  has nonlinear characteristics.

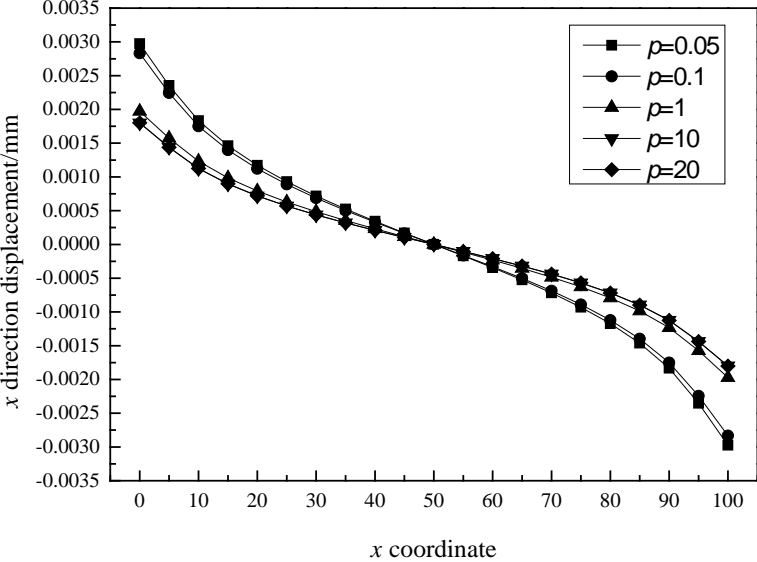


Fig. 7  $x$  direction displacement of different gradient parameters at  $y=10\text{mm}$

The displacements with different gradient parameters are shown in figure 8 at  $y = 10\text{mm}$  in the  $x$  direction. It can be seen from figure 8, the displacement in  $y$  direction at  $y = 10\text{mm}$  with the increase of  $x$  coordinate, has the characteristics of first increases, then decreases, then increases. As the gradient parameter increases, the displacement of the same position decreases. As the gradient coefficient increases, the influence of the gradient coefficient for the displacement response decreases gradually.

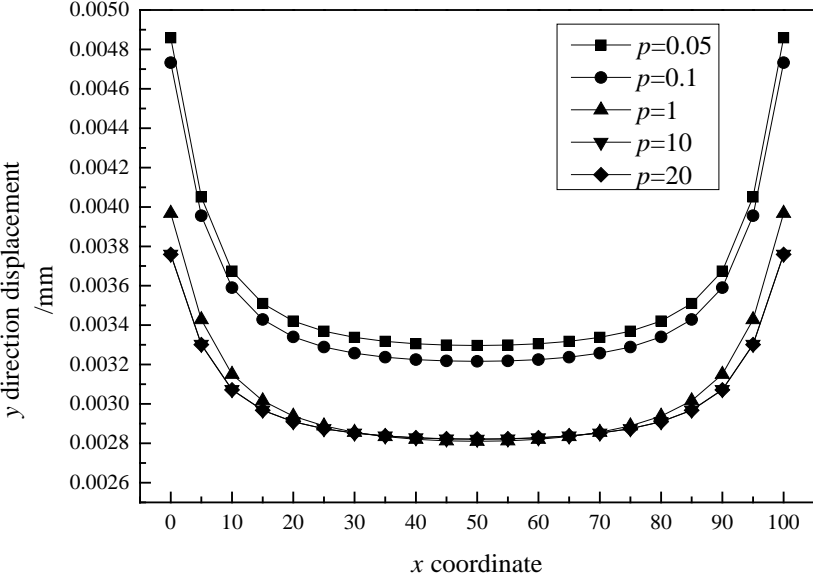


Fig. 8  $y$  directional displacement of different gradient parameters at  $y=10\text{mm}$

$x$  direction of displacement as shown in figure 9 and 10 at  $y = 50$  mm and  $y = 90$ mm. They has the same law at  $y = 50$  mm and  $y = 90$ mm. The displacement absolute value of  $x$  direction with respect to  $x = 50$ mm is symmetrical, and with the increase of gradient coefficient,  $x$  direction displacement is reduced, this is due to the increase of the gradient coefficient, the ceramics content of the material keeps increasing causing to the structure stiffness increased.

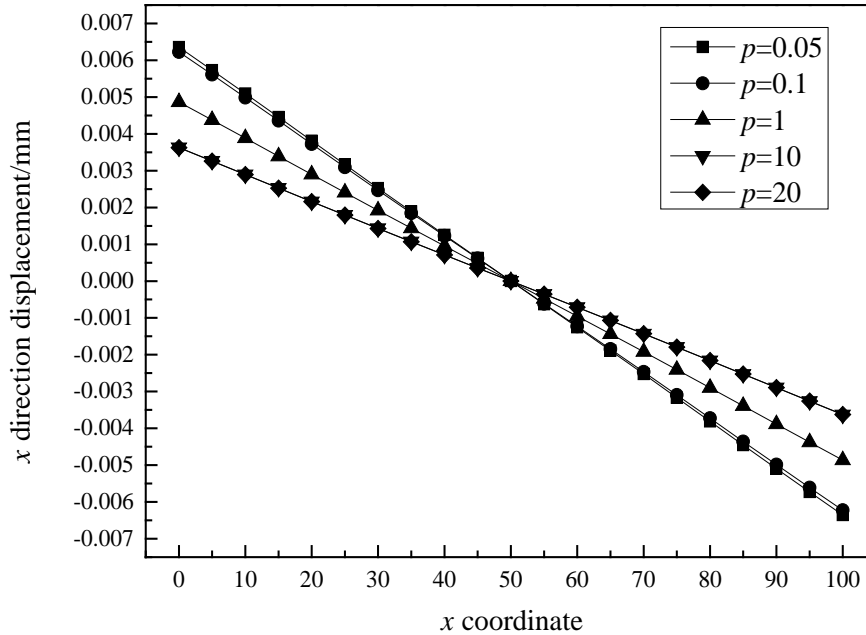


Fig. 9  $x$  directional displacement of different gradient parameters at  $y=50$ mm

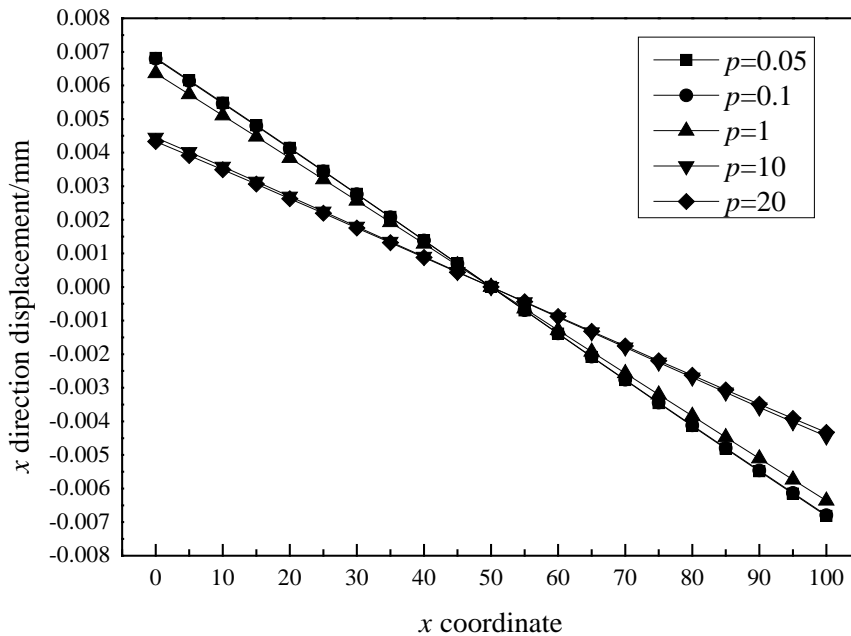


Figure 10  $x$  direction displacement for different gradient parameters at  $y=90$ mm

$y$  direction of displacement as shown in figure 11 and 12 at  $y = 50$  mm and  $y = 90$ mm. It can be seen that the displacement in  $y$  direction has class parabolic distribution, and as the change

of spatial coordinates, the change curve approximation to straight line. With the increase of gradient coefficient, structural stiffness is gradually increased, the displacement response under external loading is reduced.

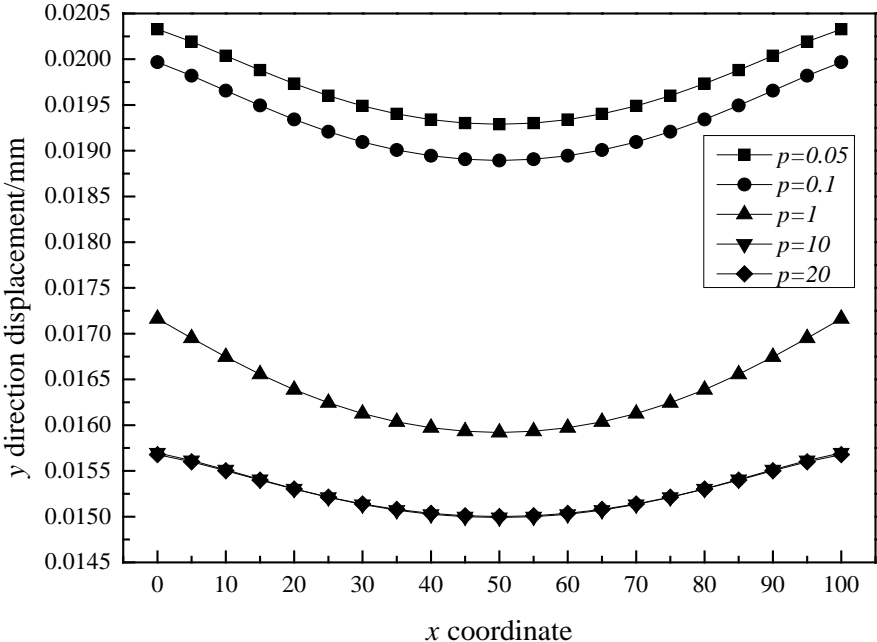


Fig. 11 y direction displacement of different gradient parameters at y=50mm

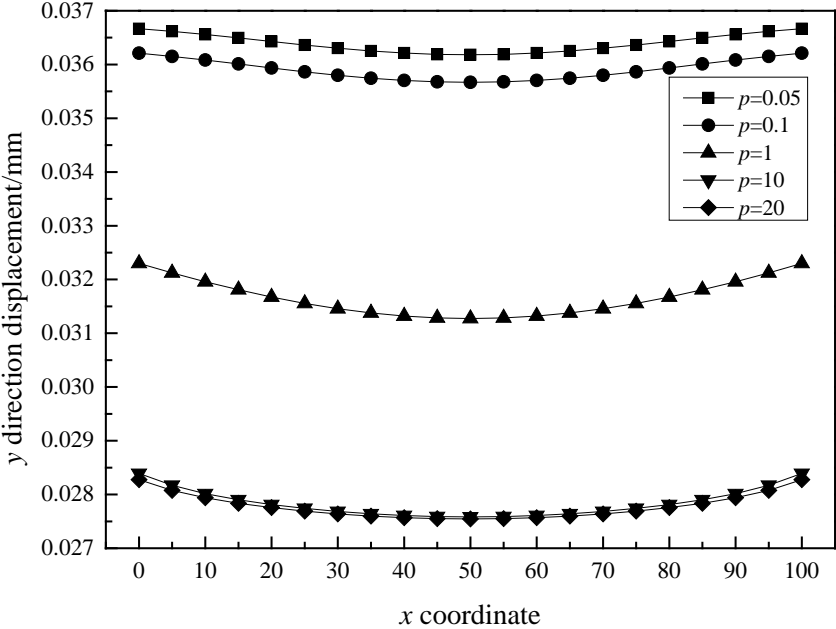


Figure 12 x direction displacement for different gradient parameters at y=90mm

**6 Conclusion**

The parameters model of the functional gradient materials is presented in this paper. The displacement response of considering different parameterized model is investigated in

mechanics loading using the strip element method, some useful results have been obtained.

1) The displacement response result is almost the same by using two methods, so to verify the validation of the strip element method.

2) With the ceramic volume fraction increases, the metal volume fraction decreases in the functionally graded materials, the structure stiffness is increasing, displacement response decreases.

3) As the gradient coefficient increases, the influence of the gradient coefficient on the structure displacement response decreases gradually.

### **Acknowledgements**

The present paper is financially supported by The National Natural Science Foundation of China (11302159), Young Talent fund of University Association for Science and Technology in Shaanxi , China(No. 20170519), and the Principal Foundation of Xi'an Technological University(No.XAGDXJJ16009).

### **Reference**

- [1] Birman V. Modeling and Analysis of Functionally Graded Materials and Structures[J]. *Applied Mechanics Reviews*, 2007, 60(5): 195-216.
- [2] Zhong Zhen, Wu Linzhi, Chen Weiqiu. Progress in the Study on Mechanics Problems of Functionally Graded Materials and Structures[J]. *Advances in Mechanics*, 2010, 40(5): 528-541.
- [3] Cao Zhiyuan. Unified Expression of Natural Frequency Solutions for Functionally Graded Composite Rectangular Plates Under Various Boundary Conditions[J]. *Acta Materiae Compositae Sinica*, 2005, 22(5): 172-177.
- [4] Liu Wuxiang. Two-dimensional Thermoelasticity Vibration Analysis of Functionally Graded Plate for Arbitrary Graded Distribution[J]. *Journal of Jiangsu University(Natural Science Edition)*, 2014, 35(3): 284-289.
- [5] CAO Zhiyuan. Analytical Solution of Dynamic Character for Functionally Graded Material Parallelogrammic Plates with Various Boundary Conditions[J]. *Chinese Quarterly of Mechanics*, 2006, 27(2): 255-261.
- [6] Reddy J N. Analysis of Functionally Graded Plates[J]. *International Journal for Numerical Methods in Engineering*, 2010, 47(47): 663-684.
- [7] Thai H T, Choi D H. A Simple First-Order Shear Deformation Theory for the Bending and Free Vibration Analysis of Functionally Graded Plates[J]. *Composite Structures*, 2013, 101(15): 332-340.
- [8] Liew K M, He X Q, Kitipornchai S. Finite Element Method for the Feedback Control of FGM shells in the Frequency Domain Via Piezoelectric Sensors and Actuators[J]. *Computer Methods in Applied Mechanics & Engineering*, 2004, 193(3-5): 257-273.
- [9] Zenkour A M. A Comprehensive Analysis of Functionally Graded Sandwich Plates: Part 1-Deflection and Stresses[J]. *International Journal of Solids & Structures*, 2005, 42(18): 5224-5242.
- [10] Ferreira A J M, Batra R C, Roque C M C, et al. Static Analysis of Functionally Graded Plates Using Third-Order Shear Deformation Theory and a Meshless Method[J]. *Composite Structures*, 2005, 69(4): 449-457.
- [11] Reddy J N, Chin C D. Thermomechanical Analysis of Functionally Graded Cylinders And Plates[J]. *Journal of Thermal Stresses*, 1998, 21(6): 593-626.
- [12] Brischetto S, Carrera E. Advanced Mixed Theories for Bending Analysis of Functionally Graded Plates[J]. *Computers & Structures*, 2010, 88(23-24): 1474-1483.
- [13] Ray M C, Sachade H M. Finite Element Analysis of Smart Functionally Graded Plates[J]. *International Journal of Solids & Structures*, 2006, 43(18-19): 5468-5484.
- [14] Kulikov G M, Plotnikova S V. A Sampling Surfaces Method and its Implementation for 3D Thermal Stress Analysis of Functionally Graded Plates[J]. *Composite Structures*, 2015, 120(10): 315-325.
- [15] Liu G R, Achenbach J D. A Strip Element Method for Stress Analysis of Anisotropic Linearly Elastic Solids[J]. *Journal of Applied Mechanics*, 1994, 61(2): 270-277.
- [16] Tian Jianhui, Han Xu , Sun Xiaowei. Transient Thermal Response of Functionally Graded Material Plates Based on the Hybrid Numerical Method[J]. *Chinese Journal of Solid Mechanics*, 2008, 29(4): 396-401.